Fabrication of polypyrrole (PPy) nanotube electrode for supercapacitors with enhanced electrochemical performance

Xuyan Liu[1] · Jiaxing Yang[1] · Xuyang Li[1] · Qiang Li[1] · Yijie Xia[1]

Abstract

PPy nanotubes were successfully fabricated by a simple situ polymerization method, using $FeCl_3$ as oxidant, methyl orange (MO) formed by the role of micelles as a guide and soft template. By varying the ratio of oxidant to pyrrole (Py) monomer, the best nanotube structure is obtained when the ratio of Py is 0.5 (mark this specimen as A_3). Moreover, the electrochemical properties of PPy nanotube electrode are investigated by cyclic voltammetry (CV), galvanostatic charge/discharge (GCD) and electrochemical impedance spectroscopy (EIS). A_3 exhibits excellent cycle performance and electrochemical performance. Meanwhile, the specific capacitance of sample A_3 is 281.2 F g^{-1} at a current density of 1 A g^{-1} and can still retain about 78% after 1000 cycles.

1 Introduction

To satisfy the growing demand in renewable sources for portable electronics and hybrid electric vehicles, it is of significant importance to develop high-performance and practicable energy storage devices [1, 2]. Lithium ion batteries and supercapacitors are two of the most promising directions and are widely used as energy storage devices. Even though the lithium ion battery can provide high energy density, there is a disadvantage of low power density [3, 4]. Compared with lithium ion batteries, supercapacitors have the advantages of fast charging, high energy density and power density, long service life, wide operating temperature range and no environmental pollution to make up for the lack of lithium batteries and ordinary capacitors [5, 6]. Currently, the main electrode materials for supercapacitor contain metal oxides, carbon and conductive polymers. The use of transition metal oxides such as RuO_x, NiO_x and MnO_x has been reported over a long period of time. Among them, RuO_x has the advantages of a wide potential window of highly reversible redox reactions, remarkably high specific capacitance, long cycle life and metallic-type conductivity. RuOx is expensive, and its performance is limited in an aqueous electrolyte [7–9].

However, the conductive polymer electrode materials, such as polypyrrole (PPy), polyaniline (PANI) and polythiophene, provide flexible mechanical behavior and excellent electrochemical oxidation and reduction property [10–12]. Among these polymers, PPy is the favorite specie because of its good environmental stability, low toxicity, high conductivity and excellent redox property [13].

Supercapacitors have been developed to close the gap between conventional capacitors and batteries, because of their high energy density and power density capabilities, such as in digital communication and electric vehicles that require electrical energy at high power levels in relatively short pulses [14, 15]. Polypyrrole consists of π-bond macromolecular chain structure composed of single and double bonds. This structure gives polypyrrole excellent performance, but also brings some disadvantages, such as lower capacitance and poor cycling stability, which limit its further application for high-performance supercapacitors. Therefore, in order to further improve the performance of polypyrrole, the well control of the PPy morphology to achieve desirable nanostructures has been recognized as one of the effective approaches to significantly enhance the capacitance and cycle performance. Recently, nanostructured conducting polymers have been developed for the electrode materials for the redox supercapacitors [16]. However, the research had been mainly focused on the nanostructured polyaniline and few work on the polypyrrole nanomaterials as the electrode materials for the redox supercapacitors was reported [17–20]. Fortunately, considerable efforts

✉ Xuyan Liu
lxuyan@163.com

[1] School of Mechanical Engineering, University of Shanghai for Science and Technology, No 516, Jun Gong Road, Shanghai 200093, China

have been devoted to the morphology-controlled synthesis of nanostructured PPy in the past decades. In particular, PPy with one-dimensional nanostructures, such as nanotubes, nanofibers, nanowires and nanorods, is regarded as favorable structures for supercapacitor because of their uniform oriented structure and larger specific surface area, which can afford a shorter pathway for ions diffusion and electron transfer [21, 22]. Sahoo et al. [23] have synthesized PPy nanofiber through a facile chemical route using sodium alginate (SA) as template. Oh and co-workers [24] developed an efficient, easily scalable method for preparation of highly porous SWNT-PPy nanocomposite electrodes suitable for industrial supercapacitor applications. This method is an extension of conventional bucky-paper fabrication method for the multi-component system, and the composites exhibited quite high specific capacitance. It was already demonstrated that nanostructure indeed can significantly affect the electrochemical properties of the active electrodes materials. The overall electrochemical properties not only depend on the structural factors but also the size and morphology of the active electrodes materials. Compared with the bulk phase materials, one-dimensional nanostructure is far easier to achieve transmission of the ions and/or charges.

In this article, PPy nanotubes were fabricated via a simple situ polymerization method, using $FeCl_3$ as oxidant, methyl orange (MO) formed by the role of micelles as a guide and soft template. Our main aim is to through the synthesis of nanostructures improve the stability of the polypyrrole electrode material, increase its specific surface area and conductivity. As we expected, further investigation demonstrated that the material has excellent electrochemical properties.

2 Experimental

2.1 Materials and methods

2.1.1 Materials

Pyrrole (Aladdin Reagent Co., Ltd., China) was used as a monomer for nanofiber preparation. Ferric chloride ($FeCl_3$, Sinopharm Chemical Reagent Co., Ltd., China) and methyl orange (MO, Sinopharm Chemical Reagent Co., Ltd., China) were used as oxidants and templating agents for the synthesis of PPy nanotubes, respectively. All of the chemical reagents used were A.R. grade. Pyrrole monomer was distilled under reduced pressure before being used.

2.1.2 Preparation of the PPy nanotube samples

Methyl orange of 0.098 g was dissolved in 150 ml of deionized water and sonicated for 1 h to obtain an orange-red solution. Then, the mixture was stirred in an ice-water bath for 30 min, 0.5 ml of Py monomer was added to the above solution and stirred for 1 h, marked as solution A. A certain amount of $FeCl_3$ was dissolved in 50 ml of deionized water and stirred for 30 min, marked as solution B. Solution B was placed in a constant pressure dropping funnel and slowly added to solution A. The mixed solution was stirred in an ice-water bath for 24 h to obtain a black reaction solution. The resulting solution was suction filtered until the filtrate was colorless and neutral. After drying under vacuum at 40 °C for 24 h, a dark powdery solid was obtained. $FeCl_3$ and polypyrrole monomer ratio were 1, 0.8, 0.5, 0.3, respectively; the preparation of the samples was recorded as A_1, A_2, A_3, A_4, samples without dopant template MO recorded as A_0.

2.2 Characterizations

The morphology of PPy nanotube was analyzed through SEM instrument (JSM-6700F, 5.0 kV, Japan). Small amount of sample was adhered to the sample holder by carbon tape and analyzed by SEM. However, before analysis the samples were sputtered with gold in order to make them conducting. PPy nanotube was characterized by XRD (Bruker D-8 Avance, Cu Ka radiation; 1 ¼ 1.5418 Å) measurements with a scan step of 5° and a scan range from 20° to 80°.

2.3 Electrochemical performance measurements

The model half batteries were assembled in an argon-filled glovebox (omni-LAB, VC, USA).The mass of PPy layer was obtained after measuring the mass of 1.14 cm^2 Cu substrate coated with PPy layer and a 1.14 cm^2 Cu bare substrate. The discharge–charge cycling was performed at room temperature by using a multichannel battery tester (LANHE, CT2001A, China). Cyclic voltammetric (CV) measurements were performed at different scanning rates within the range of 0–0.7 V in room temperature. Electrochemical impedance was recorded with electrochemical impedance spectroscopy over the frequency range of 100 kHz to 0.01 Hz.

3 Results and discussion

The SEM images of polypyrrole nanotubes synthesized with methyl orange as template and $FeCl_3$ as oxidant at different $FeCl_3$ concentrations and SEM images of polypyrrole synthesized without template MO are shown in Fig. 1. As shown in Fig. 1, the PPy nanotubes in a large area are formed in different $FeCl_3$ concentrations when methyl orange MO is used as a template, and the nanotubes are interconnected to form a close-packed network structure. And the morphology of the polypyrrole nanotubes synthesized under various $FeCl_3$ concentrations using methyl orange as a template
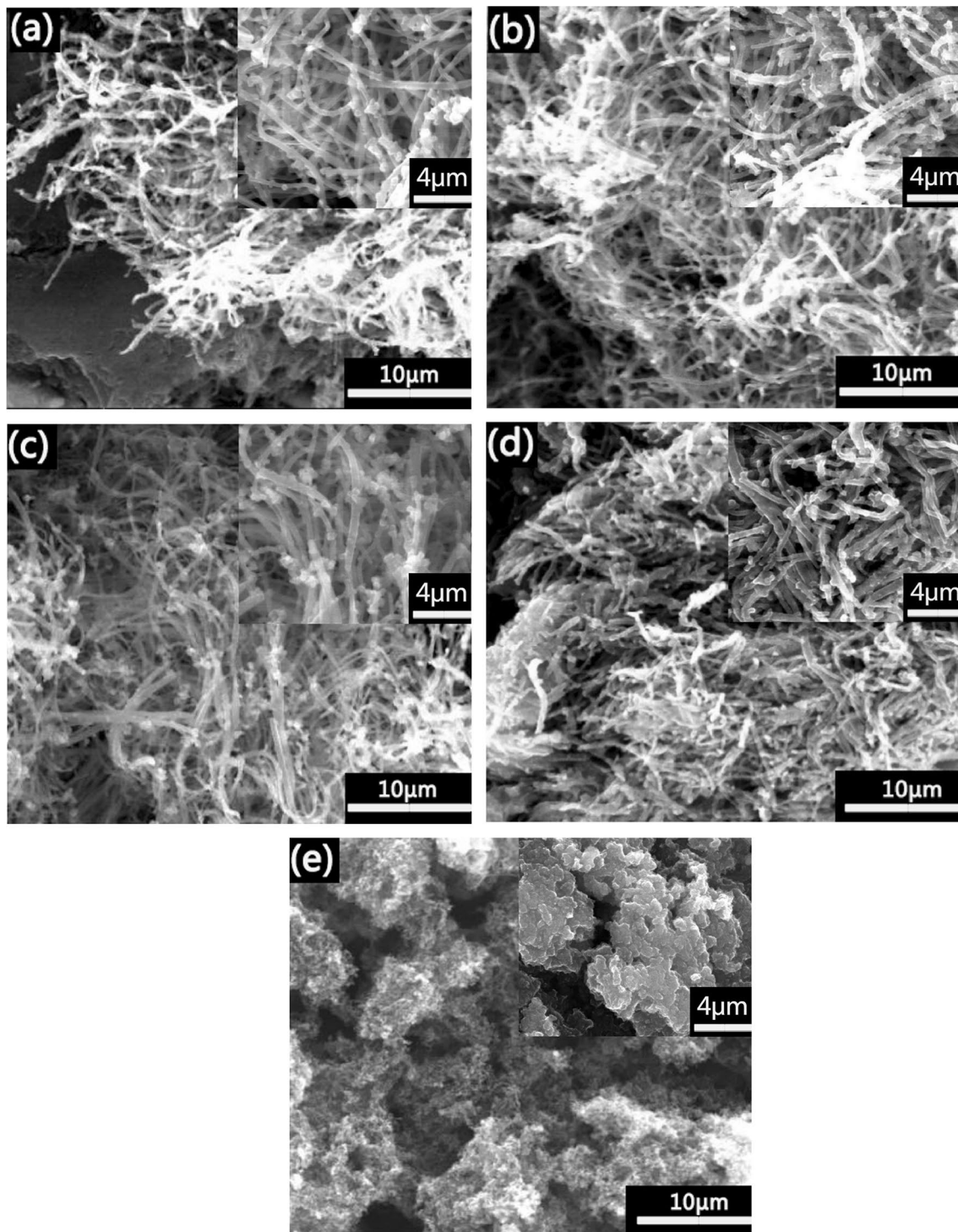
Fig. 1 SEM images of polypyrrole synthesized under different concentrations of $FeCl_3$ and SEM images of PPy without template, **a** A_1, **b** A_2, **c** A_3, **d** A_4 and **e** A_0

shows a nanotube shape, and the morphology of the nanotubes is relatively regular. Figure 1e is the SEM image of synthesized polypyrrole without template MO doping. It can be seen from the images that in the absence of the template

MO, the flower-like or granular PPy, but cannot get the tubular structure of PPy. By comparing the microstructure of synthesized PPy with and without template MO, we can conclude that MO acts as a fibrous template and plays a decisive

role in the microstructure of PPy synthesized. At the same time, polypyrrole nanotubes were observed to have a rough surface at higher magnification with better dispersibility.

Figure 2 is an XRD image of PPy prepared with different concentrations of $FeCl_3$ oxidant and PPy synthesized without template. The main results are compared with the XRD image of samples A_1, A_2, A_3, A_4 and sample A_0. According to the XRD image of A_1, A_2, A_3, A_4 and A_0, it can be seen that there are two obvious characteristic peaks and amorphous dispersion peaks of polypyrrole. The two characteristic peaks are located at 16° and 26°, indicating that amorphous polypyrrole was indeed synthesized in the experiment. Comparing the XRD image of synthesized samples, it can be seen that there is a diffraction peak of A_1, A_2, A_3, A_4 and A_0 at 44°. The diffraction peak of A_2 and A_3 is obvious, and the diffraction peak of A_0, A_1 and A_4 is relatively not obvious. It shows that when the ratio of $FeCl_3$ and Py monomer is 0.5, the order of polypyrrole is higher. Based on the intensity of the characteristic diffraction peak, it can be inferred that the conductivity of A_3 is better than that of A_2 [25]. At the same time, the XRD image of polypyrrole with or without template synthesis was analyzed. It can be seen that the presence of methyl orange increased the regularity of PPy chain and further improved the ordering of PPy, which was in good agreement with the prepared polypyrrole's tubular microstructure being consistent [26].

Figure 3 shows the CV curves of PPy prepared at different amounts of oxidizer as the material of the supercapacitor electrode. After several tests, it can be seen that the CV curve of the PPy nanotubes in the range of 0–0.7 V is the closest to the rectangle, that is to say the electrochemical performance is optimized. Therefore, the
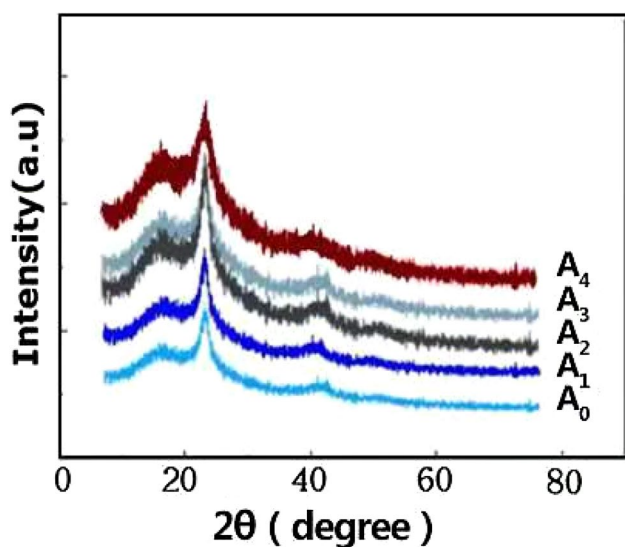
cyclic voltammetry test conditions are as follows: voltage window 0–0.7 V, scan rates were 5 mV/s, 10 mV/s, 30 mV/s, 50 mV/s, 100 mV/s. In this experiment, we mainly compared the CV curves of samples A_2, A_3 and A_4 synthesized with methyl orange as a template and sample A_0 without template synthesis. From the CV curves of samples A_2, A_3, A_4 and A_0, we can see that the CV curves of the PPy nanotubes have the same rectangular shape and no obvious redox peaks, which proves that PPy nanotubes have good charge–discharge reversibility and fast ion-exchange behavior as electrode materials of supercapacitors. For the same electrode material, the specific capacity decreases with the increase in scan rate. At the same time, comparing the CV curve of sample A_0 with samples A_2, A_3, A_4 with methyl orange as a template, it can be seen that the CV curve of PPy synthesized with methyl orange is better than that without template the CV curve of synthesized PPy, which shows that PPy synthesized by using methyl orange as template has better cycle stability. In addition, a careful comparison of the three CV curves of samples A_2, A_3 and A_4 synthesized using methyl orange as a template shows that when the ratio of oxidant to Py is 0.5, the area enclosed by the CV curve is the largest, which has the largest capacitance and the A_3 exhibited better cycle stability.

Figure 4 shows the galvanostatic charge–discharge (GCD) curve of sample A_3 prepared at a 0.5 ratio of oxidant to Py monomer. The test conditions of the GCD are as follows: the voltage window is 0–0.7 V, and the charge–discharge current densities are 1 A g^{-1}, 2 A g^{-1} and 3 A g^{-1}, respectively. From the GCD curve of sample A_3 at different current densities, it can be seen that there is a linear relationship between the voltage and the time in the sample A_3 when it is charged and discharged at a constant current density. Therefore, sample A_3 has good capacitance performance as electrode material in the supercapacitor. At the same time, by comparing GCD curves at different current densities, it can be seen that the capacitance of sample A_3 increases with decreasing current density. The specific capacitance of sample A_3 was 281.2 F g^{-1} at a current density of 1 A g^{-1}. Figure 5 shows the GCD curves of samples A_3 and A_0 at a current density of 1 A g^{-1}. By comparing the constant current charge and discharge curves of the samples A_0 and A_3 at the same current density, we can clearly see that the sample A_3 synthesized by the template has a higher doping level than the sample A_0 synthesized without the template. The tubular structure increases the specific surface area of PPy, accelerates the entry and exit of electrolyte ions and thus enhances the capacitive properties of PPy. The results show that the capacitive properties of PPy synthesized with template MO are better than that of PPy synthesized without template. After constant current charge–discharge cycle test, sample A_3 had a constant
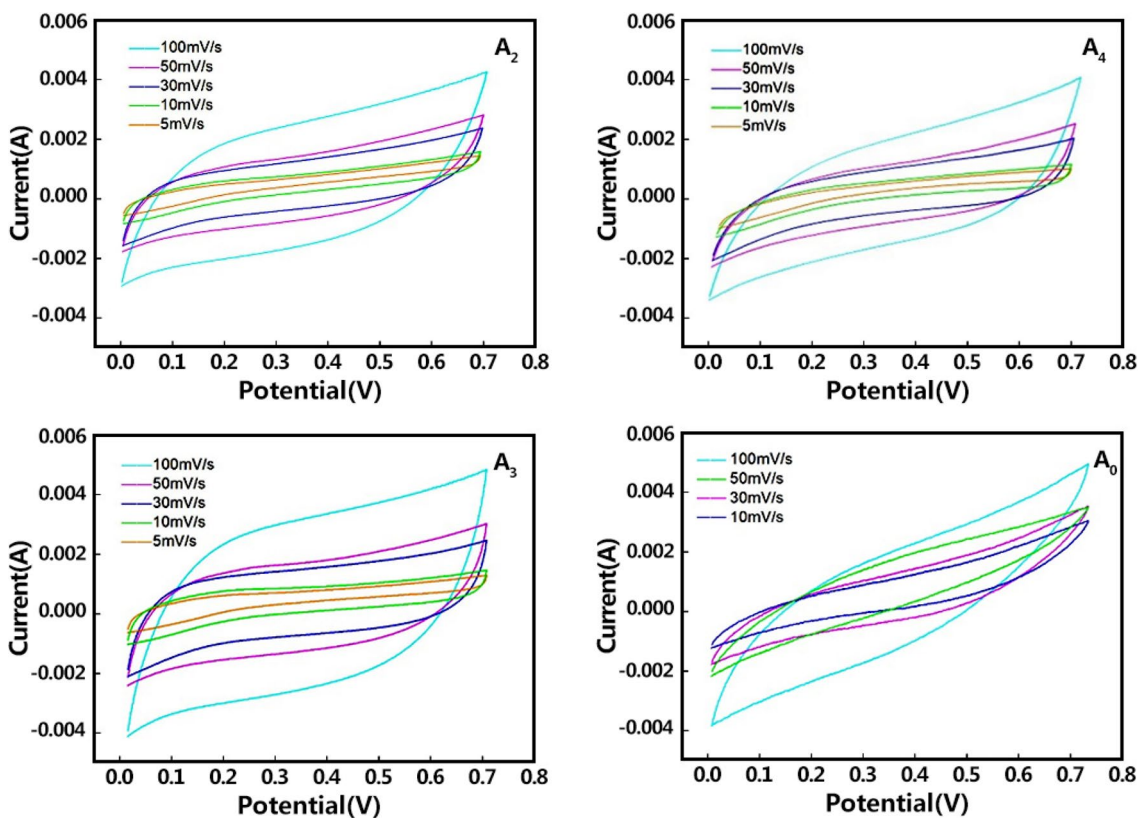
Fig. 2 XRD image of samples A_1, A_2, A_3, A_4 and A_0

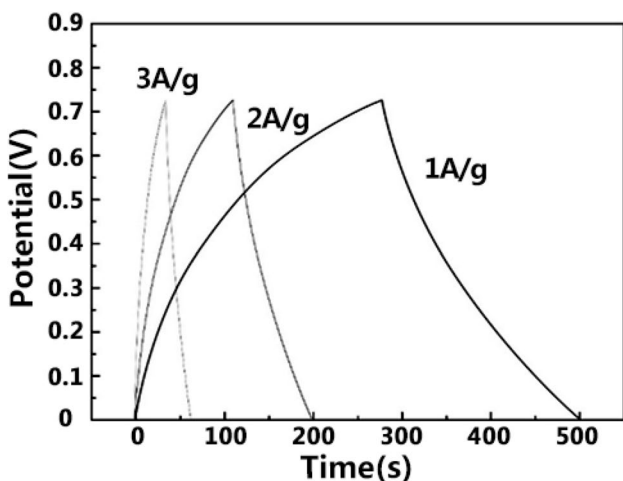**Fig. 3** The CV curves of PPy prepared from different concentrations of FeCl$_3$

Fig. 4 GCD curve of sample A$_3$ at different current densities
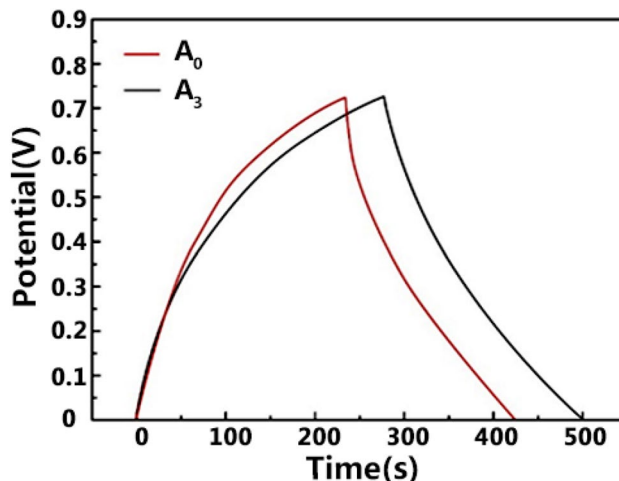

Fig. 5 GCD curve comparison of samples A$_0$ and A$_3$ (current density 1 A g^{-1})

current charge–discharge cycle of 1000 times at a current density of 1 A g^{-1}, and its specific capacitance was still about 78%. Under the same conditions, the sample A$_0$ retention rate is of about 70%. Therefore, sample A$_3$ using methyl orange as a template has better electrochemical stability than sample A$_0$ without template.

The electrochemical impedance spectroscopy (EIS) and equivalent circuit diagrams of samples A$_3$ and A$_0$ are shown in Fig. 6. In the high-frequency range, the EIS curve of the sample appears semicircular shape, while the internal resistance of the supercapacitor is the size of the intercept
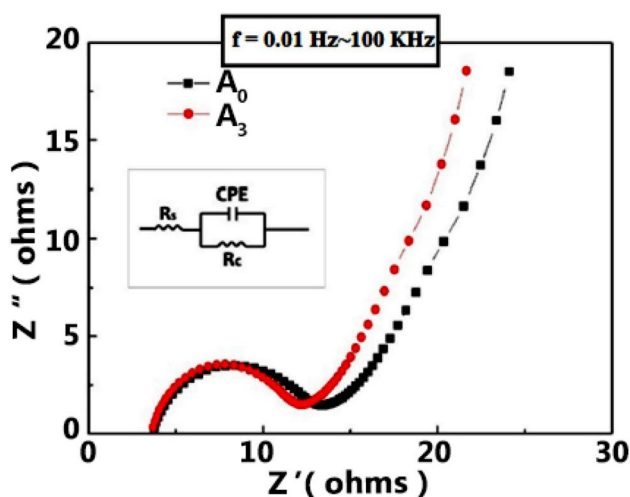
Fig. 6 Electrochemical impedance curves of samples A_0 and A_3

between the semicircle and the horizontal axis of the coordinate system. In the low-frequency range, the EIS curve is an approximate straight-line whose slope reflects the capacitive behavior of the supercapacitor. The larger the slope, the greater the rate of ion exchange, and the better the electrochemical performance of the measured supercapacitor. By comparing the EIS curves of samples A_3 and A_0, it can be seen that both sample A_3 and A_0 show an approximate straight-line with a large slope in the low-frequency range. A_0 and A_3 have excellent electrochemical performance as electrode materials. The slope of the EIS curve of sample A_3 is larger, indicating that the ion-exchange behavior of sample A_3 is faster and the capacitance is better.

4 Conclusion

In the field of supercapacitor, electrode materials with different nanostructures are one of the most effective methods to improve electrochemical performance. We have proposed a simple ecofriendly synthetic procedure to prepare PPy nanotube by using MO as a soft template. By contrast with other PPy-based electrodes, the PPy nanotube electrode shows good electrochemical property in cyclic voltammetry and galvanostatic charge/discharge measurements. The excellent electrochemical performance and the excellent cycle stability would lead the PPy nanotube electrode to be a promising material for making electrodes of polymer supercapacitors.

References

1. J.P. Holdren, Science **315**, 30–34 (2007)
2. X.C. Wang, W. Jia, Y.D. Huang et al., J. Mater. Chem. A **4**, 13907–13915 (2016)
3. W.J. Si, X.Z. Wu, W. Xing et al., J. Inorg. Mater. **26**, 107–113 (2011)
4. C.M. Niu, E.K. Sichel, R. Hoch et al., Appl. Phys. Lett. **70**(11), 1480–1482 (1997)
5. R. Ramya, R. Sivasubramanian, M.V. Sangaranarayanan, Electrochim. Acta **101**, 109–129 (2013)
6. X. Zheng, J. Luo, W. Lv et al., Adv. Mater. **27**(36), 5388–5395 (2015)
7. Z.T. Meng, Y.D. Huang, Y.C. Fang, J. Alloy. Compd. **784**, 620–627 (2019)
8. C.C. Hu, M.J. Liu, K.H. Chang, J. Power Sources **163**(2), 1126–1131 (2007)
9. U.M. Patil, R.R. Salunkhe, K.V. Gurav, C.D. Lokhande, Appl. Surf. Sci. **255**, 2603–2607 (2008)
10. W. Sun, X.Y. Chen, J. Power Sources **193**(2), 924–929 (2009)
11. H. Zhou, H. Chen, S. Luo, G. Lu, W. Wei, Y. Kuan, J. Solid State Electrochem. **9**(8), 574–580 (2005)
12. A. Laforgue, P. Simon, C. Sarrazin, J. Power Sources **80**, 142–148 (1999)
13. N. Ballav, M. Biswas, Mater. Lett. **60**, 514–517 (2006)
14. S.J. Bao, B.L. He, Y.Y. Liang, W.J. Zhou, H.L. Li, Mater. Sci. Eng., A **397**, 305–309 (2005)
15. Y.G. Wang, X.G. Zhang, Electrochim. Acta **49**, 1957–1962 (2004)
16. A. Malinauskas, J. Malinauskiene, A. Ramanavicius, Nanotechnology **16**, 51–62 (2005)
17. X. Lang, Q. Wan, C. Feng, X. Yue, W. Xu, J. Li, S. Fan, Synth. Met. **160**, 1800–1804 (2010)
18. J.Y. Woo, G.C. Liu, J.K. Lee et al., ACS Nano **12**(6), 5588–5604 (2018)
19. S. Lee, M.S. Cho, J.D. Nam, Y. Lee, J. Nanosci. Nanotechnol. **8**, 5036–5041 (2008)
20. J.Y. Kim, G.C. Liu, J.K. Lee et al., ACS Appl. Mater. Interfaces **10**(10), 8692–8701 (2018)
21. S. Sahoo, S. Dhibar, G. Hatui, P. Bhattacharya, Polymer **54**(3), 1033–1042 (2013)
22. A. Pruna, Q. Shao, M. Kamruzzaman, J.A. Zapien, A. Ruotolo, Electrochim. Acta **187**, 517–524 (2016)
23. S. Sahoo, Express Polym. Lett. **6**(12), 965–974 (2012)
24. J. Oh, M.E. Kozlov, B.G. Kim, H.-K. Kim, R.H. Baughman, Y.H. Hwang, Synth. Met. **158**, 638–641 (2008)
25. M.X. Wan, J.C. Li, J. Polym. Sci., Part A: Polym. Chem. **38**, 2359–2364 (2000)
26. P.M. Carrasco, H.J. Grande, M. Cortazar et al., J. Synth. Met. **156**(5–6), 420–425 (2006)